JACS
JOURNAL OF THE AMERICAN CHEMICAL SOCIETY
Article
pubs.acs.org/JACS

Manipulating Magnetism: Ru_2^{5+} Paddlewheels Devoid of Axial Interactions

Gina M. Chiarella,[†] F. Albert Cotton,[†,§] Carlos A. Murillo,*[,†] Karen Ventura,[‡] Dino Villagrán,*[,‡] and Xiaoping Wang[†,⊥]

[†]Department of Chemistry, Texas A&M University, P.O. Box 30012, College Station, Texas 77842-3012, United States
[‡]Department of Chemistry, University of Texas at El Paso, El Paso, Texas 79968, United States

Supporting Information

ABSTRACT: Variable-temperature magnetic and structural data of two pairs of diruthenium isomers, one pair having an axial ligand and the formula $Ru_2(DArF)_4Cl$ (where DArF is the anion of a diarylformamidine isomer and Ar = *p*-anisyl or *m*-anisyl) and the other one being essentially identical but devoid of axial ligands and having the formula $[Ru_2(DArF)_4]BF_4$, show that the axial ligand has a significant effect on the electronic structure of the diruthenium unit. Variable temperature crystallographic and magnetic data as well as density functional theory calculations unequivocally demonstrate the occurrence of π interactions between the p orbitals of the chlorine ligand and the π^* orbitals in the Ru_2^{5+} units. The magnetic and structural data are consistent with the existence of combined ligand σ/metal σ and ligand pπ/metal-dπ interactions. Electron paramagnetic resonance data show unambiguously that the unpaired electrons are in metal-based molecular orbitals.

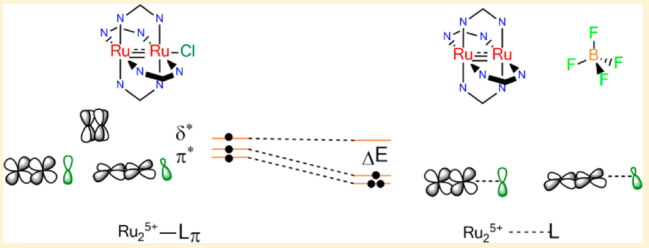

INTRODUCTION

While the occurrence of π interactions between ligand and metal atoms has long been known to occur,[1] it is not often that unambigous evidence can be found, especially in complexes containing transition metal species. Here we describe much evidence to support their effect, albeit found in a nontraditional place, that is, diruthenium paddlewheel compounds with metal−metal bonds.

Reports from our laboratories[2] have drawn attention to the way in which structural data over a wide temperature range can provide valuable information and heretofore unutilized evidence pertaining to electronic structures, in particular, those of paddlewheel compounds having Ru_2^{5+} cores. One of the enticing but frustrating features of such compounds, of which the earliest were of the type $Ru_2(O_2CR)_4Cl$,[3] is that their frontier molecular orbitals are usually very similar in energy.[4,5] Even small variations in their relative energies can lead to significant changes in their electronic structure, which affects the corresponding metal−metal distances[5,6] and magnetism.[7] Because of the similarity in energy between the highest occupied molecular orbital (HOMO) and the singly occupied molecular orbital (SOMO), the provenance of the ground state for these species with an 11-electron core might be any of three configurations, $Q\delta^{*2}\pi^*$, $Q\pi^{*2}\delta^*$, $Q\pi^{*3}$ (where Q represents the underlying $\sigma^2\pi^4\delta^2$ quadruple bond configuration).[8] Moreover, two states that each arise from a different one of these configurations (which have bond orders of 2.5) might be so close in energy that a Boltzmann-type temperature dependence of their partial populations could come into play. For these configurations, magnetic measurements may distinguish between the $Q\pi^{*2}\delta^*$ state, which has three unpaired electrons, but not the other two states ($Q\delta^{*2}\pi^*$ and $Q\pi^{*3}$), which have one unpaired electron each.

The temperature dependence, or absence thereof, of the Ru−Ru bond length can show whether or not close-lying states that derive from different configurations are involved, and if so, which pairs of configurations are pertinent. For example,[2b] the combination of the magnetic and structural data for $Ru_2(DAni^pF)_4Cl$, **1**, ($DAni^pF$ = *N*,*N*′-di-*p*-anisylformamidinate shown in Scheme 1) lead to the certain conclusion that there is a ground state (^2E_g) derived from the $Q\pi^{*3}$ configuration (11 metal-centered electrons) and a low-lying excited state ($^4B_{2u}$)

Scheme 1. Line Drawings of Some of the Ligands Cited in the Text

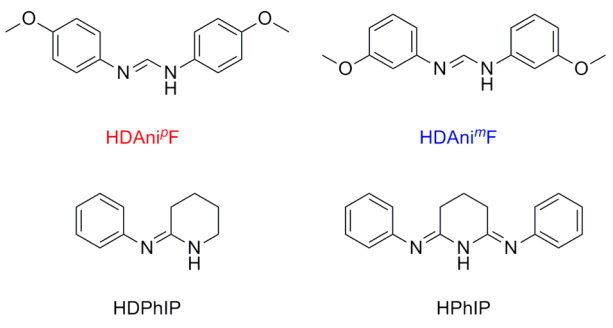

Received: March 4, 2014
Published: May 30, 2014

   dx.doi.org/10.1021/ja5020647 | J. Am. Chem. Soc. 2014, 136, 9580−9589

derived from the $Q\pi^{*2}\delta^{*}$ configuration (Scheme 2). In the same report it was shown that for the meta isomer

Scheme 2. Electronic Splitting Diagram for an 11 e^- Bimetallic Unit with an Idealized D_{4h} Symmetry

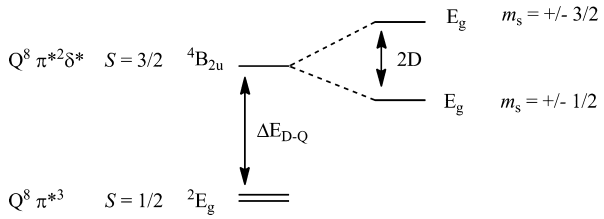

$Ru_2(DAni^mF)_4Cl$, **2**, where the ligand is less basic than that of the para isomer, the $Q\pi^{*2}\delta^{*}$ configuration persists at all temperatures between 27 and 300 K. Although there is a strong temperature dependence of the magnetism due to zero-field splitting (ZFS), in which the magnetism seemingly drops from an equivalent of three unpaired electrons to an apparent state with only one unpaired electron, the Ru−Ru distance is essentially temperature-independent. An axial chlorine atom is present in both of these isomers, and it was only the basicity of the DArF ligands (where DArF is the anion of a diarylformamidine isomer, and Ar = *p*-anisyl or *m*-anisyl) in **1** and **2** that changed. It should also be mentioned that in another crystal having two crystallographically distinct but chemically similar molecules with Ru_2^{5+} cores and slightly different intermolecular interactions to axial ligands, the two molecules behaved very differently as the temperature was lowered. The Ru−Ru distances changed for one of the molecules but not for the other molecule.[9]

Here the consequences of two other variations in compounds of the $Ru_2(DArF)_4X$ type are explored (DArF = *N*,*N*′-diarylformamidinate): (1) what happens when the same DArF bridges are retained, but the axial chloride species are replaced by the essentially noncoordinating BF_4^- anion;[10] and (2) what happens when the aryl group (Ar) in DArF is changed from *p*-Ani to *m*-Ani (Ani = anisyl) in $[Ru_2(DArF)_4]BF_4$ to form two species devoid of axial coordination, namely, $[Ru_2(DAni^pF)_4]BF_4$, **3**, and $[Ru_2(DAni^mF)_4]BF_4$, **4**. The existence of pairs of compounds with identical cores for which one of the members of the pair has an axial ligand while the other one is naked allows for the first time an unambiguous analysis of the effect of axial ligation in Ru_2^{5+} species. As discussed below, the results are consistent with significant π interactions of the axial Cl groups with the diruthenium units in the $Ru_2(DArF)_4Cl$ species.

RESULTS AND DISCUSSION

Syntheses. The preparation of the $Ru_2(DArF)_4Cl$ compounds **1** and **2** was accomplished in tetrahydrofuran (THF) by the reaction of $Ru_2(OAc)_4Cl$ with the corresponding diarylformamidine in the presence of triethylamine to aid the deprotonation process and anhydrous LiCl to promote the ligand substitution reaction. Substitution of the axial chlorine atoms from the $Ru_2(DArF)_4Cl$ compounds to produce **3** and **4** was carried out by the addition of a solution of $TlBF_4$ in the noncoordinating solvent CH_2Cl_2,[11] followed by removal of the insoluble thallium chloride:

$$Ru_2(O_2CCH_3)_4Cl + 4HDArF + LiCl \rightarrow Ru_2(DArF)_4Cl + 4HO_2CCH_3$$

$$Ru_2(DArF)_4Cl + TlBF_4 \rightarrow [Ru_2(DArF)_4]BF_4 + TlCl$$

Structure and Magnetism. As noted, the substitution of the axial groups in $Ru_2(DArF)_4Cl$ type compounds by noncoordinating anions in the absence of other possible coordinating species allows for exploration of the consequences of two other variations in compounds of the $Ru_2(DArF)_4X$ type: (1) the effect of the same DArF bridges being retained while the axial chloride species are replaced by the essentially noncoordinating BF_4^- anion; and (2) the effect of small basicity effects of the Ar being changed from *p*-Ani to *m*-Ani in $[Ru_2(DArF)_4]BF_4$ isomers.[12]

Variation (1). Structures of $[Ru_2(DAni^pF)_4]BF_4$, **3**, one of which is shown in the upper section of Figure 1, were

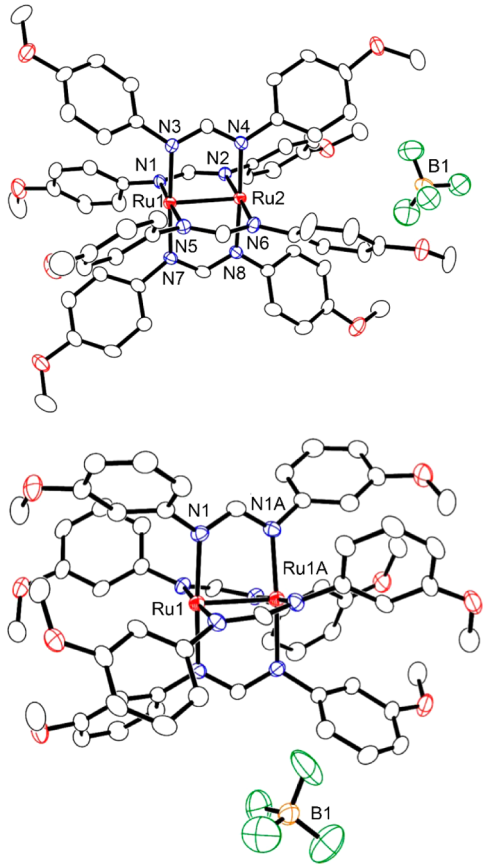

Figure 1. Crystal structures at 213 K of the isomers $[Ru_2(DAni^pF)_4]BF_4$ (**3**, top) and $[Ru_2(DAni^mF)_4]BF_4$ (**4**, bottom) drawn with displacement ellipsoids at the 30% probability level. Hydrogen and disordered atoms have been omitted for clarity.

determined at 27, 200, and 298 K, and principal bond lengths at each of those temperatures are provided in Table 1. The Ru−Ru distance is in the range of 2.4000(5)−2.4078(7) Å at all measured temperatures, and this is consistent with the structure of the Ru_2N_8 core in **3** being temperature-independent. These results contrast those for **1**,[2b] where the Ru−Ru distance decreased by about 0.05 Å, from 2.4471(5) Å at 27 K to 2.3968(5) Å at 300 K (Table 2). The cation in **3**, which is devoid of axial interactions,[13] represents the first structurally

dx.doi.org/10.1021/ja5020647 | J. Am. Chem. Soc. 2014, 136, 9580−9589

Table 1. Selected Bond Distances and Angles for 3 at Three Temperatures

	3[a]	3[b]	3[c]
Ru1−Ru2	2.4078(7)	2.4069(7)	2.4000(5)
Ru1−N8	2.038	2.038	2.029
Ru1−Ru2−N4	88.9	88.8	88.8
Ru2−Ru1−N4	88.7	88.7	88.9

[a]27 K. [b]200 K. [c]298 K.

Table 2. Ru−Ru Bond Distances for 1 and 2 at Different Temperatures[a]

temperature (K)	1	2[b]
27	2.4471(5)	2.3333(3)
60	2.4397(6)	
100	2.4289(5)	2.3326(3)
150	2.4168(5)	
220	2.4019(5)	2.3376(3)[c]
299	2.3968(5)	2.3398(4)

[a]See ref 2a. [b]Data at 60 and 150 K were not collected. [c]Collected at 213 K.

characterized example of a naked Ru_2^{5+} paddlewheel compound.[14]

Structures for $[Ru_2(DAni^mF)_4]BF_4$, **4**, one of which is shown at the bottom of Figure 1, were determined at 33, 100, 200, and 298 K. Again, the Ru−Ru distance in the cation remains constant and in the range of 2.389(4)−2.3839(4) Å. Selected results of the variable-temperature (VT) crystallographic studies are shown in Table 3 and Figure 2. Similarly to **3**, it

Table 3. Selected Bond Distances and Angles for 4 at Different Temperatures

	4[a]	4[b]	4[c]	4[d]
Ru1−Ru1A	2.389(4)	2.383(4)	2.3879(19)	2.3859(14)
Ru1−N1	2.065(7)	2.041(7)	2.035(5)	2.033(4)
Ru1−Ru1A−N1	88.2(2)	87.8(2)	88.18(15)	88.30(11)

[a]33 K. [b]100 K. [c]213 K. [d]298 K.

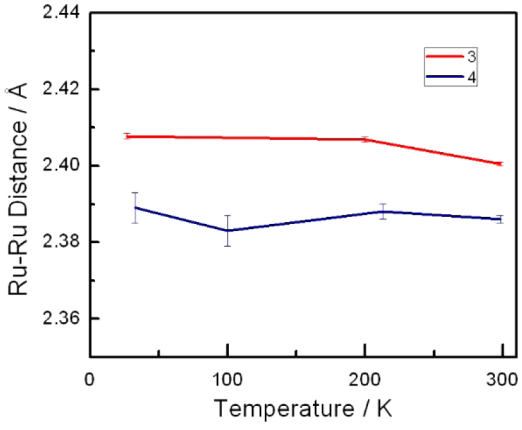

Figure 2. Change in Ru−Ru distances for **3** and **4**. The distances remain basically constant within the margin of error in the measured range of temperatures.

is again clear that the structure of this axially naked species is temperature-independent, and thus its electronic structure is invariant with respect to temperature. In this aspect, **4** resembles the axially chlorine-ligated **2**; however, the corresponding Ru−Ru distance varies by ∼0.05 Å, with that of **2** being shorter than that of **4**.

The magnetism of **3** is consistent with an $S = {}^1/_2$ state over the range of 2 K to ambient temperature, as shown in Figure 3.

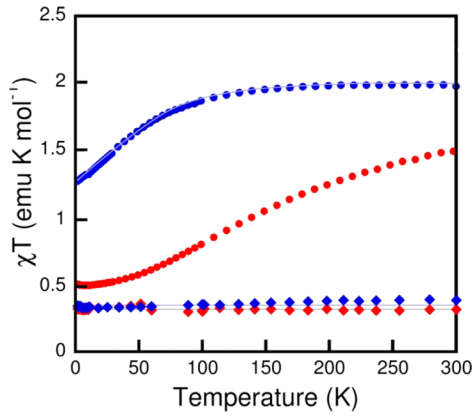

Figure 3. Magnetic susceptibility versus temperature of $Ru_2(DAni^pF)_4Cl$ (**1**, red circles), $Ru_2(DAni^mF)_4Cl$ (**2**, blue circles), $[Ru_2(DAni^pF)_4]BF_4$ (**3**, red diamonds), and $[Ru_2(DAni^mF)_4]BF_4$ (**4**, blue diamonds).

This is also in sharp contrast to that of **1**, which shows three unpaired electrons at room temperature with a χT value that reaches a maximum of 1.6 emu·K·mol^{-1} at 300 K and declines to a minimum of 0.5 emu·K·mol^{-1} at 2 K (red circles in Figure 3). This behavior has been attributed to a spin-crossover process from a doublet ground-state derived from a $Q\pi^{*3}$ configuration at low temperatures to a spin quartet state derived from a $Q\pi^{*2}\delta^*$ configuration.[2b] The magnetism of **3** also differs from that of **2**, which follows a commonly observed decrease in the χT value attributable to ZFS for a $^4B_{2u}$ state derived from a $Q\pi^{*2}\delta$ configuration (Scheme 2) that is frequent in Ru_2^{5+} species.[7a,15,16] For **4**, the magnetism resembles that of **3** also having one unpaired electron and the χT value being constant (0.35 ± 0.02 emu·K·mol^{-1}) from 2 to 300 K. This data can be modeled by the Curie law ($\chi = ((Ng^2\beta^2)/(3kT))S(S + 1)$) with fitted values of g of 1.925(4) and 2.000(5) for **1** and **2**, respectively, where N is Avogadro's number, β is the Bohr magneton, k is the Boltzmann constant, and T is the temperature in Kelvin.

To explain the difference in structural and magnetic properties of **1** and **3**, the interactions of the axial chloride ion in **1** with the Ru_2^{5+} core must be considered. The structural and magnetic data suggest that **1**, at low temperature, and **3** at all measured temperatures are in the ^2E_g state arising from the $Q\pi^{*3}$ configuration (Scheme 2). The reason that **1** has a longer Ru−Ru distance in this state is because, as is commonly found in paddlewheel compounds with metal−metal bonds,[5] an axial σ donor weakens the metal−metal σ bonding. The fact that **3** remains in the ^2E_g state as the temperature rises to 300 K indicates that the separation between the ^2E_g state and the lowest state arising from the $Q\pi^{*2}\delta^*$ configuration (Scheme 2) is above the value of kT at 300 K (i.e., ≥ 600 cm^{-1}). Contrarily, this separation must be smaller in **1** than in **3**. The reason for this difference in magnetism must be attributed to a destabilization of energy of the π^* orbitals by the axial Cl^- ligand attached to the $[Ru_2(DAni^pF)_4]^+$ core while (because of

dx.doi.org/10.1021/ja5020647 | J. Am. Chem. Soc. 2014, 136, 9580−9589

Table 4. Electronic Configurations for Some Related Ru_2^{5+} Complexes

	1 Cl/para	3 BF_4/para	2 Cl/meta	4 BF_4/meta	5 Cl/D(3,5-Cl_2Ph)F[a]	6 Cl/Pr^nCO_2	$[Ru_2(DPhF)_3(OAc)$-$(CH_3CN)]BF_4$[b]	$Ru_2(DPhF)_3$-(OAc)Cl
Ru−Ru (Å)	2.4471(5) (27 K) 2.3968(5) (298 K)	2.4078(7) (27 K) 2.4000(5) (298 K)	2.333(3) (27 K) 2.3398(4) (298 K)	2.389(4) (33K) 2.3859(4) (298 K)	2.360(1) (27 K) 2.368(1) (300 K)	2.281(4)	2.4131(5)	2.3248(13)
electronic configuration	π^{*3} ($\rightarrow\pi^{*2}\delta^*$)	π^{*3}	$\pi^{*2}\delta^*$	π^{*3}	$\pi^{*2}\delta^*$	$\pi^{*2}\delta^*$	π^{*3}	$\pi^{*2}\delta^*$
Ru−Cl (Å)					2.38	2.59		
Ru−Cl′ or Ru−OH_2 (Å)					2.63	2.59		
ref	2b	this work	2b	this work	7e	3b	29	28

[a] $[Ru_2(D(3,5\text{-}Cl_2Ph)F)_4Cl(0.5H_2O)]\cdot C_6H_{14}$, where D(3,5-$Cl_2$Ph)F = the anion of *N*,*N*′-di(3,5-dichlorophenyl)formamidine. [b] DPhF = the anion of *N*,*N*′-diphenylformamidine.

symmetry incompatibility) there is no direct effect on the δ^* orbital.

The difference in Ru−Ru bond distances between **2** and **4** can be explained by invoking a similar argument. These compounds have different electronic configurations, $Q\pi^{*2}\delta^*$ and $Q\pi^{*3}$ for **2** and **4**, respectively. Because a π^* orbital has a greater antibonding character than does a δ^* orbital, the $Q\pi^{*3}$ configuration is expected to be more repulsive than that in the $Q\pi^{*2}\delta^*$ configuration, and thus the Ru−Ru distance in **4** is longer than that in **2**.

Variation (2). When there is no significant axial ligation as in both of the $[Ru_2(DArF)_4]BF_4$ species **3** and **4**, the change from the more basic DAni^{p}F to the less basic DAni^{m}F[12] has no major effect on the structure and magnetism. Nonetheless, there is a slight decrease of 0.019 Å in the Ru−Ru distance from 2.4069(7) in **3** at 200 K to 2.3879(19) Å in **4** at 213 K, but this distance is temperature-independent in both compounds. This result coupled with the fact that in each case χT is also temperature-independent and corresponds to one unpaired electron suggests that in each case a $Q\pi^{*2}\delta^*$ ground state as well as any temperature-dependent distribution over two states can be ruled out. The only remaining possibilities are that (1) a ^2E_g state arises from a π^{*3} configuration in both cases, or that (2) a $^2B_{2u}$ state arises from a $\delta^{*2}\pi^*$ configuration in the two cases.

To decide between these two possibilities, the structure of the BF_4 compounds must be compared to those of the corresponding Cl compounds. In making these comparisons, we shall invoke two principal modes of interaction of the axial Cl^- ion with the Ru_2^{5+} core: (1) a σ donor interaction that should weaken and hence lengthen the Ru−Ru bond and (2) a π donor interaction that will lower the energy of the π^* orbitals.

In the comparison of **3** and **1**, the shortening of the Ru−Ru distance[17] at 27 K by about 0.044 Å can be accounted for on the basis of the first effect. On the basis of the second effect, the π^{*3} configuration would have an increased stability compared to that of the $\pi^{*2}\delta^*$ configuration, and thus the latter would remain unpopulated even at 300 K in **3**.

In the comparison of **4** and **2**, the rather large increase (0.052 Å, Table 4) in the Ru−Ru distance upon the removal of the axial Cl^- is the opposite of what the simple loss of a σ donor interaction would produce; however, an increase would result from a change from a $\pi^{*2}\delta^*$ configuration in **2** to a π^{*3} configuration in **4**. If the change in configuration from **2** to **4** were from $\pi^{*2}\delta^*$ to $\delta^{*2}\pi^*$ there would be no apparent explanation for the bond length increase since a δ^* orbital is expected to be less destabilizing than is a π^* orbital. Indeed, in one of the very few characterized compounds with an Ru_2^{5+} core having a $Q\delta^{*2}\pi^*$ electronic configuration, $Na_3[Ru_2(Cl_4Cat)_4(THF)]$, where Cl_4Cat = tetrachlorocatecholate, which has two nonbridging catecholate ligands and an axial THF molecule, the unsupported Ru−Ru distance shown in Table 4 is only 2.273(1) Å.[18] This distance decreases even further upon a one-electron oxidation that leads to the removal of the electron in the π^* orbital to 2.2233(6) Å.[18]

Electron Paramagnetic Resonance Studies. Electron paramagnetic resonance (EPR) spectra that was recorded in a toluene glass of **1**−**4** were obtained to further explore their electronic structures and the effects of their respective axial interactions. Compounds **1** and **2** are EPR silent at room temperature because of the large ZFS arising from the splitting of the $M_S = 0$ and $M_S = {}^3/_2$ Zeeman levels. This is in agreement with the observed magnetic susceptibility measurement data. At lower temperatures (10 K), highly anisotropic EPR signals were clearly discerned (Figure 4 and Figure S1 of the Supporting Information). The signal for **1** in Figure 4 shows two *g*-tensor components because of the strong axial anisotropy, suggesting that the unpaired electrons reside in anisotropic environments and also supporting the occurrence of large ZFS. The spectrum for **2** (Figure S1 of the Supporting Information) is similar to that for **1**. This suggests that **1** and **2** have similar electronic structures in solution. For **1** the effective g^e values of $g^e_\perp = 4.07$ and $g^e_\parallel = 1.94$ correspond to an isotropic *g* value of 2.00, while for **2** the effective *g* values of $g^e_\perp = 4.09$ and $g^e_\parallel = 1.94$ correspond to an isotropic *g* value of 2.01.[19] Consequently, the

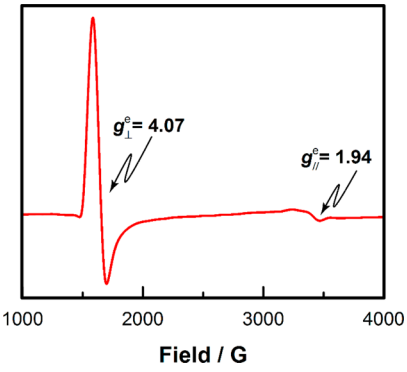

Figure 4. X-band EPR spectrum measured on a frozen toluene solution of **1** at 10 K, demonstrating that the unpaired spins are in an anisotropic environment and that the unpaired electrons are in metal-based molecular orbitals.

dx.doi.org/10.1021/ja5020647 | J. Am. Chem. Soc. 2014, 136, 9580−9589

actual values for compound **1** are $g_{\perp} = 2.035$ and $g_{\parallel} = 1.94$, and the actual values for **2** are $g_{\perp} = 2.045$ and $g_{\parallel} = 1.94$.

When the axial interactions in these isomers are removed as in **3** and **4**, the EPR signals drastically change. Figure 5 and

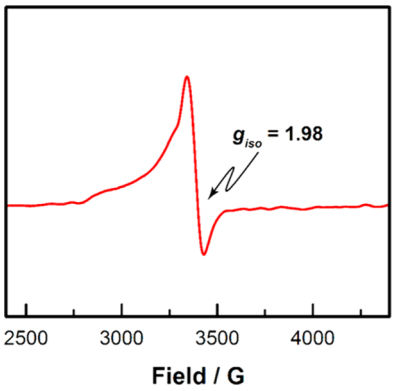

Figure 5. X-band EPR spectrum measured on a frozen toluene solution of **3** at 10 K.

Figure S2 of the Supporting Information show the low temperature EPR spectra of **3** and **4**, respectively. The spectra of **3** and **4** show only one signal at 2.01 and 1.99, respectively. According to the magnetic data (vide infra) **3** and **4** have a spin state of $S = {}^1/_2$; therefore, no ZFS is expected and only isotropic signals were indeed observed.

Comparisons to Other Dimetal Systems. Two additional well-studied dimetal cores that are affected by axial ligands are those having M_2^{4+} species, where M = Cr and Rh.[20] For Cr it was not until about a decade ago that the first $Cr_2(O_2CR)_4$ compound without axial ligands was isolated.[21] The Cr−Cr distance of 1.9662(5) Å is significantly shorter than those in other $Cr_2(O_2CR)_4L_2$ compounds, L = donating ligand, which have Cr−Cr distances about 0.4 Å longer. For the rhodium analogues, $Rh_2(O_2CR)_4L_2$, which have Rh−Rh distances in the range of 2.34−2.41 Å,[20,22] the change in the metal−metal bond is not as large, and for the compound without axial ligands this distance is 2.3499(4) Å.[23]

An additional pair of compounds that provide a relevant comparison is represented by $Cr_2(DPhIP)_4$ and $Cr_2(PhIP)_4$ (DPhIP = the anion of 2,6-di(phenylimino)piperidine and PhIP = the anion of 2-(phenylimino)piperidine, shown at the bottom of Scheme 1). Both of these paddlewheel compounds have Cr_2N_8 cores, yet the Cr−Cr distances differ by about 0.41 Å, being 2.265(1) Å in $Cr_2(DPhIP)_4$ and 1.858(1) Å in $Cr_2(PhIP)_4$.[24] This difference has been attributed to the four imino nitrogen lone pairs in the DPhIP ligands that are positioned to donate to the π^* orbital of the Cr_2^{4+} unit at distances of about 2.73 Å, while $Cr_2(PhIP)_4$ is devoid of such interactions.

More recently, an analogous effect was reported involving the axial interactions of the triple bonded $[W_2(hpp)_4]^{2+}$ dication (hpp = the anion of 1,3,4,6,7,8-hexahydro-2*H*-pyrimido[1,2-*a*]pyrimidine), which is the precursor of $W_2(hpp)_4$, a thermally stable molecule with a very low ionization energy.[25] In halogenated solvents, $W_2(hpp)_4$ is easily oxidized to $W_2(hpp)_4Cl_2$.[26] This compound has very long W···Cl distances of about 3.0 Å, but density functional theory (DFT) calculations showed that even at those long axial distances, strong repulsive interactions exist between the metal−metal and the Cl ligand $p\sigma_s$ occupied orbitals.[25] A related effect has also been observed in analogous compounds having Re_2^{6+} cores.[27]

Another pair of compounds that are pertinent to the present discussion involve $Ru_2(DPhF)_3(OAc)Cl$[28] and $[Ru_2(DPhF)_3(OAc)(acetonitrile)]BF_4$[29] (DPhF) = *N,N′*-diphenylformamidine). Both compounds have an Ru_2^{5+} core surrounded by four bridging ligands (a mix of formamidinate and acetate ligands) and a paddlewheel structure akin to **1**−**4**. The compound $Ru_2(DPhF)_3(OAc)Cl$ also has one axial halogen atom similar to those of **1** and **2**. The species $[Ru_2(DPhF)_3(OAc)(acetonitrile)]BF_4$, unlike **3** and **4** has an axial CH_3CN molecule. It should be noted that the acetonitrile molecule is a good σ donor but not a good π donor, and this explains why the Ru−Ru distance in the acetonitrile compound increases by about 0.09 Å (Table 4) relative to that of the chlorine-containing compound. This is consistent with the hypothesis provided in the Variation (2) section above. It should be noted that Jiménez-Aparicio et al. have also reported on a series of additional $Ru_2(DPhF)_3(OAc)L_{ax}$, where L_{ax} = $OPMe_3$, H_2O, 4-picolinate, and CO that clearly shows that the nature of the axial ligand, L_{ax}, affects the Ru−Ru bond distance.[30] Some of the distances for compounds in this family are shown in Table 5.

Table 5. Distances (Å) for a Family of Paddlewheel $[Ru_2(DPhF)_3(OAc)L_{ax}]^+$ Species with Ru_2^{5+} Cores and Mixed Diphenylformaminate and Acetate Paddles[a]

L_{ax}	Ru−Ru
$OPMe_3$	2.303
Cl	2.3248
H_2O	2.350
4-picolinate	2.408
acetonitrile	2.4131
CO	2.450

[a]Note that as the π acceptor capability of the ligand (e.g., in CO) increases, the gap between the π^* and δ^* orbitals increases favoring the $Q\pi^{*3}$ electronic configuration. This lowers the magnetism and also concomitantly increases the metal-to-metal distance.[30]

DFT Calculations. To qualitatively investigate the effect of the axial interactions on the electronic structure of these $[Ru_2(DAniF)_4]^+$ systems, a series of DFT calculations based on models of the axially ligated **1** and **2** and the axially naked **3** and **4** were used, and the relative energies of the optimized geometries of the doublet and quartet multiplicities of each model were calculated. In the models, the aryl groups in the bridging formamidinate ligands were replaced by H atoms. These simplifications were done to reduce the computation expense; however, it is important to note that such simplifications do not significantly compromise the modeling of the electronic structure, as shown before.[31] Two different multiplicities (doublet and quartet) were calculated for the models of the axially chlorine-ligated species **1** and **2** and for the models of the axially naked $[Ru_2(DAniF)_4]^+$ species **3** and **4**. The calculated total energies of the geometry optimized models are given in Table 6. A comparison of the relative energies of the doublet ($S = {}^1/_2$) and quartet ($S = {}^3/_2$) states that the axially chlorine-ligated model indicates the quartet state is more stable than the doublet state by about 1.4 kcal/mol. This small energy difference is consistent with the experimentally observed behavior of **1**, which shows temperature-dependent spin-crossover.[2b] By contrast, the energy difference

dx.doi.org/10.1021/ja5020647 | *J. Am. Chem. Soc.* 2014, 136, 9580−9589

Table 6. DFT Energies for the Calculated Models

model	multiplicity	S	energy (hartrees)	ΔE_{d-q} (kcal/mol)	ΔE_{d-q} (kcal/mol)[b]
axially ligated Cl	doublet	1/2	−1245.7696034	−1.40	−2.33
	quartet	3/2	−1245.7718294		
axially naked	doublet	1/2	−785.297632398	5.44	4.50
	quartet	3/2	−785.288961454		
axially ligated with long Cl[a]	doublet	1/2	−1245.68693350	6.21	8.32
	quartet	3/2	−1245.67703316		

[a]Not geometry optimized but using the axially naked geometry. [b]Energies calculated with the Couty−Hall modified LANL basis set.[45]

between the doublet and the quartet states in the axially devoid model shows that the doublet state is favored over the quartet state by about 5.4 kcal/mol as shown in Table 6.[32] This is a significantly larger energy difference than that was calculated for the axially chlorine-ligated model and is consistent with the observed magnetism of **3** and **4**, which shows a doublet state at all temperatures. This energy difference between the doublet and quartet states from the two different systems (axially ligated and naked) suggests that the doublet state is stabilized by the removal of the axial Cl^- anion. As mentioned earlier, this axial ligand interaction on Ru_2^{5+} systems had been previously noted.[30] Our calculations of the naked paddlewheel Ru_2^{5+} system support previous results, but the current calculations go beyond what has been done so far. The current set of calculations was carried out by manipulating the distances from the Ru atom to the axial Cl^- anion (either by shortening or lengthening them). In this way, it is possible to track the metal orbital energies as a function of the axial $Ru_2\cdots L_{ax}$ separation.

A qualitative diagrammatic representation of the metal−metal bonding manifold corresponding to the long and short axial Cl ligand distances is given in Scheme 3. On the left of the

Scheme 3. Molecular Orbital Diagram[a]

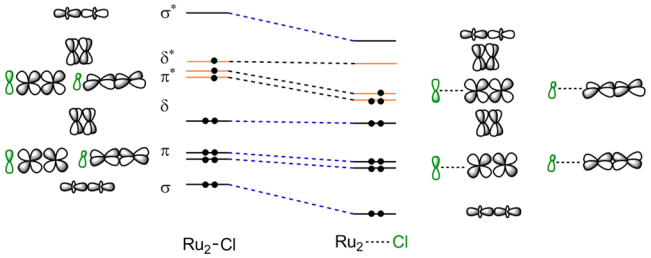

[a]As the Ru···Cl separation increases, the energy of the metal-based π orbitals quickly drops, increasing the $\pi-\delta$ gap. The diagram depicts a short Ru_2-Cl interaction on the left, and a long $Ru_2\cdots Cl$ interaction on the right.

diagram the frontier orbitals (δ^* and π^*) show a quasi-degeneracy, but this quasi-degeneracy is broken as the axial Cl atom is removed (right). This effect is due to antibonding interactions between the Cl p orbitals and the orbitals of π symmetry of the diruthenium core. As the Cl anion leaves the axial site, the π^* metal−metal orbital is stabilized.[33] A quantitative estimate of the extent of this π^*orbital stabilization can be obtained by comparing the relative energies of the frontier orbitals of the axially Cl^- ligated model and a second calculation that uses the optimized geometry of the axially naked Ru_2 model. In this model, the Cl^- anion was positioned at a distance of 8.0 Å from the diruthenium unit where no chemically meaningful $Ru_2\cdots Cl$ interaction would be expected. For this model, and consistent with the results from the axially naked one, the doublet state is more stable than the quartet state by 6.21 kcal/mol (Table 6). Figure 6 shows a molecular

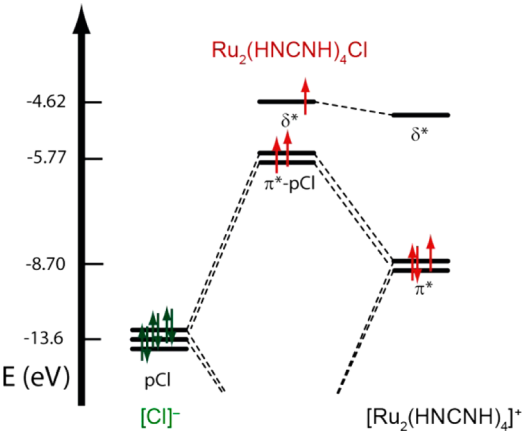

Figure 6. Molecular orbital diagram showing the construction of the frontier orbitals of the Cl^- axially ligated model from the axially naked Ru_2^{5+} core and Cl^- ligand p orbitals. Note that the energy gap between the metal-based π^* and δ^* orbitals significantly increases from $Ru_2(DArF)_4Cl$ to that in the naked cation $[Ru_2(DArF)_4]^+$.

orbital diagram constructed from the calculations of the ground state models at two different $Ru_2\cdots Cl$ separations. The quartet state model (depicted by the molecular orbitals (MOs) at the center of Figure 6) shows that the metal-based π^* orbitals are about 1 eV more stable than the δ^* orbitals. As the chlorine atom is pulled away (Figure 6, outer MOs), the energy separation between the π^* and δ^* orbitals increases to about 4.0 eV. Because of the long $Ru_2\cdots Cl$ distances in the doublet state case, the p_{Cl} orbitals are isolated, and thus have energies similar to those expected for an outer sphere Cl^- anion. Figure 6 also shows that the metal-based π^* orbitals of the model with the long $Ru_2\cdots Cl$ separations are more stable in energy (by about 2.9 eV) than those with the shorter separations. Even though the δ^* orbital is also stabilized by the $Ru_2\cdots Cl$ elongation, the drop in energy is relatively small compared to that of the π^* orbitals and thus the energy separation between the π^* and δ^* orbitals increases to 4.0 eV. Therefore, the calculations for the model with the long $Ru_2\cdots Cl$ distances favor the doublet state by about 6.21 kcal/mol. In contrast, calculations for the model with the short $Ru_2\cdots Cl$ distances favor the quartet state, mainly because of the smaller $\pi^*-\delta^*$ energy separation of ∼1 eV.[34] This is consistent with the observed magnetism of **1** and **2**, which have short Ru_2-Cl distances and accessible quartet states and contrasts with the observed magnetism of **3** and **4**, which show only an accessible doublet state at all temperatures and no $Ru-L_{ax}$ interactions.

dx.doi.org/10.1021/ja5020647 | J. Am. Chem. Soc. 2014, 136, 9580−9589

CONCLUSIONS

The isolation of a pair of diruthenium compounds having the same core but very different axial interactions has allowed us to obtain important insight into the electronic structures of Ru_2^{5+} cores. These compounds show that there is a significant impact of metal−ligand π interactions in the electronic structure of metal systems that is responsible for changes in various physical properties. Specifically, the removal of axial interactions in Ru_2^{5+} systems allows for the manipulation of the magnetism. DFT calculations support the ground states observed by magnetic measurements and confirm the qualitative MO picture predicted by the MO theory. The magnetic and structural data are consistent with the existence of combined ligand σ/metal σ and ligand pπ/metal-dπ interactions. The confirmation and isolation of this type of interactions may lead to significant advances in the control of magnetic behavior.

EXPERIMENTAL SECTION

Unless otherwise noted, all syntheses were carried out under an inert atmosphere using standard Schlenk techniques. The ligand precursors HDAni^{p}F and HDAni^{m}F were prepared by the general thermolysis reaction of triethylorthoformate in the presence of the corresponding aniline at 130 °C over 4 h, followed by the extensive washing of the solids with pentane before their use.[35] The diruthenium $Ru_2(OAc)_4Cl$ precursor was prepared as previously reported.[36] Compound **1** was prepared according to an established synthetic procedure.[37] Solvents were dried using a Glass Contour solvent system. Elemental analyses were performed by Robertson Microlit Laboratories, Inc., Madison, NJ. Infrared spectra were recorded in a PerkinElmer 16PC FT-IR spectrophotometer using KBr pellets. The X-band (~9.5 GHz) variable-temperature EPR spectra were obtained using a BrukerEMX-plus spectrometer with an ER073 magnet and equipped with a cryogen-free 10° FlexLine system. All samples were measured in frozen toluene (glasses) at 10 K. To increase the solubility of **2** and **4** in toluene, a couple of drops of dichloromethane were added to the EPR samples. Variable-temperature magnetic susceptibility measurements were obtained from 2 to 300 K using a Quantum Design SQUID magnetometer MPMS-XL operated at 1000 G. These data were corrected for diamagnetism using Pascal's constants.[38]

Synthesis of $[Ru_2(DAni^{m}F)_4]Cl$, 2. In a 100 mL round-bottomed flask equipped with a condenser and a magnetic stirring bar, $Ru_2(OAc)_4Cl$ (0.961 g, 2.00 mmol), HDAni^{m}F (4.10 g, 16.0 mmol), triethylamine (5 mL), and an excess of anhydrous LiCl (2.0 g) were mixed in 50 mL of THF that had been degassed via freeze−thawing. The mixture was heated to reflux under nitrogen for 48 h. The solvent from the dark green mixture was then removed under a vacuum. The solid was washed with water to remove LiCl and then extracted with CH_2Cl_2 and further purified using a silica gel column and a mixture of hexanes, CH_2Cl_2, and acetone as eluent. From this point on, the compound was no longer protected from the air. A fraction contained in a dark band was collected, and the solvent was then removed under a vacuum to produce 2.36 g of a green solid. Yield: 85%. Crystals suitable for X-ray analysis were obtained by the slow diffusion of hexanes into a CH_2Cl_2 solution of the product. Anal. Calcd for $C_{60}H_{60}N_8O_8ClRu_2$: C, 57.25; H, 4.80; N, 8.90%. Found: C, 57.61; H, 4.80; N, 8.71%. IR (KBr pellet, cm^{-1}): 1600, 1534, 1482, 1466, 1327, 1283, 1265, 1195, 1152, 1081 (BF_4^-), 1038, 983, 939, 858, 774, 757, 695, 522, 449.

Synthesis of $[Ru_2(DAni^{p}F)_4]BF_4$, 3. To a solution of $Ru_2(DAni^{p}F)_4Cl$ (0.255 g, 0.200 mmol) in 20 mL of CH_2Cl_2 was added a stoichiometric amount of $TlBF_4$. The mixture was stirred overnight at room temperature. The mixture was then filtered through Celite to remove the insoluble TlCl. The volume of the bluish solution was reduced to about 5 mL and then layered with hexanes to yield single crystals of X-ray diffraction quality. Anal. Calcd for $C_{60}H_{60}N_8O_8BF_4Ru_2$: C, 55.01; H, 4.62; N, 8.55%. Found: C, 54.77;

Table 7. Crystallographic Data for 3 and 4

	3	3	3	4	4	4	4
chemical formula	$Ru_2C_{60}H_{60}N_8O_8BF_4$	$Ru_2C_{60}H_{60}N_8O_8BF_4$	$Ru_2C_{60}H_{60}N_8O_8BF_4$	$Ru_2C_{60}H_{60}N_8O_8BF_4$	$Ru_2C_{60}H_{60}N_8O_8BF_4$	$Ru_2C_{60}H_{60}N_8O_8BF_4$	$Ru_2C_{60}H_{60}N_8O_8BF_4$
formula weight	1310.11	1310.11	1310.11	1310.11	1310.11	1310.11	1310.11
space group	$Pna2_1$ (No. 33)	$Pna2_1$ (No. 33)	$Pna2_1$ (No. 33)	$P4/nnc$ (No. 126)	$P4/nnc$ (No. 126)	$P4/nnc$ (No. 126)	$P4/nnc$ (No. 126)
a (Å)	34.572(6)	34.973(8)	34.973(8)	13.7952(18)	13.6662(11)	13.7952(18)	13.8927(5)
b (Å)	12.945(2)	13.011(3)	13.011(3)	13.7952(18)	13.6662(11)	13.7952(18)	13.8927(5)
c (Å)	12.682(2)	12.766(3)	12.766(3)	15.095(3)	15.052(2)	15.095(3)	15.0744(11)
V (Å^3)	5675.3(17)	5809(2)	5809(2)	2872.7(8)	2811.3(6)	2872.7(8)	2909.5(3)
Z	4	4	4	2	2	2	2
d_{calc} (g·cm^{-3})	1.533	1.498	1.498	1.515	1.548	1.515	1.495
μ (mm^{-1})	0.609	0.595	0.595	0.601	0.614	0.601	0.594
T (K)	27(2)	200(2)	298(2)	33(2)	100(2)	213(2)	298(2)
$R1^a$ ($wR2^b$)	0.0595 (0.1272)	0.0390 (0.0823)	0.0441 (0.0848)	0.1222 (0.2218)	0.0983 (0.2062)	0.0719 (0.1649)	0.0541 (0.1408)

$^aR1 = [\sum w(F_o - F_c)^2/\sum wF_o^2]^{1/2}$. $^bwR2 = [\sum w(F_o^2 - F_c^2)^2/\sum w(F_o^2)^2]^{1/2}$, $w = 1/[\sigma^2(F_o^2) + (aP)^2 + bP]$, where $P = [\max(F_o^2,0) + 2(F_c^2)]/3$.

dx.doi.org/10.1021/ja5020647 | J. Am. Chem. Soc. 2014, 136, 9580−9589

H, 4.43; N, 8.61%. IR (ATR, cm^{-1}): 1605, 1496, 1459, 1392, 1253, 1186, 1081 (BF_4^-), 1030, 724, 693.

Synthesis of $[Ru_2(DAni^mF)_4]BF_4$, 4. A salt metathesis reaction similar to that used for the synthesis of **3** was utilized. Yield: 93%. Anal. Calcd for $C_{60}H_{60}N_8O_8BF_4Ru_2$: C, 55.01; H, 4.62; N, 8.55%. Found: C, 54.66; H, 4.61; N, 8.29%. IR (KBr pellet, cm^{-1}): 1582, 1522, 1482, 1444, 1305, 1287, 1265, 1197, 1156, 1083, 1056 (BF_4^-), 1039, 985, 943, 845, 762, 691.

Computational Details. DFT[39] calculations were performed with the hybrid Becke-3[40] parameter exchange functional and the Lee–Yang–Parr[41] nonlocal correlation functional (B3LYP) as implemented in the Gaussian 03 program suite.[42] Double-ζ-quality basis sets (D95)[43] were used on nonmetal atoms (carbon, nitrogen, and hydrogen) except for Cl (6-311g(d)). An effective core potential (ECP)[44] representing the 1s2s2p3s3p3d core was used for the ruthenium atoms along with the associated double-ζ basis set (LANL2DZ). A second set of calculations using the modified version of LANL2DZ by Couty and Hall to the ruthenium atoms was applied for redundancy and comparison.[45] The convergence criterion for the self-consistent field cycles on all calculations was increased from the default value to 10^{-8}. Geometry optimization calculations were found to be minima in the potential energy surface as evidenced by the lack of imaginary vibrations in the frequency calculations.

X-ray Structure Determinations. Crystals of **3** and **4** were coated with Paratone oil and mounted on a nylon Cryoloop that was affixed to a goniometer head. Data for **3** and **4** were collected on a Bruker SMART 1000 charge-coupled device (CCD) area detector system using omega scans of 0.3 deg per frame, with exposures of 30, 10, and 10 s per frame at 27, 200, and 298 K, respectively. The exposure rates for **4** were 20 s per frame at the temperatures of 33, 100, 213, and 298 K. Cell parameters were determined using the SMART software suite.[46] Data reduction and integration were performed with the software SAINT.[47] Absorption corrections were applied using the program SADABS.[48] The positions of the Ru atoms were found via direct methods using the program SHELXTL.[49] Subsequent cycles of least-squares refinement followed by difference Fourier syntheses revealed the positions of the remaining non-hydrogen atoms. Hydrogen atoms were added in idealized positions. All hydrogen atoms were included in the calculation of the structure factors. All non-hydrogen atoms were refined with anisotropic displacement parameters. In **3**, half of the atoms in the $DAni^pF$ ligands were disordered. The disorder in the four ligands was successfully treated with a major component varying from 74.9–79.8% and a minor component of 20.2–25.1% depending on the temperature at which the data were collected. The tetrafluoroborate anion was also disordered and the structure was refined in the orthorhombic space group $Pna2_1$. For **4**, the structure refinement was done in the tetragonal space group $P4/nnc$ instead of the lower-symmetry space group $P4/n$ that was suggested by the XPREP program. This was done following Marsh's recommendations.[50] Data collection and refinement parameters for **3** and **4** are summarized in Table 7. Selected bond distances and angles are listed in Tables 1 and 3.

■ ASSOCIATED CONTENT

Ⓢ Supporting Information

X-ray crystallographic data in CIF format for **3** at 27, 200, and 298 K; for **4** at 33, 100, 213, and 298 K; EPR data for **2**; and a graphical representation of the molecular orbitals for the model $Ru_2(HNCNH)_4Cl$ in PDF format. This material is available free of charge via the Internet at http://pubs.acs.org.

■ AUTHOR INFORMATION

Corresponding Authors

murillo@tamu.edu
dino@utep.edu

Present Address

[⊥]Chemical and Engineering Materials Division, Oak Ridge National Laboratory, PO Box 2008 MS6475, Oak Ridge, TN 37831, United States.

Notes

The authors declare no competing financial interest.
[§]Deceased, February 20, 2007.

■ ACKNOWLEDGMENTS

This work was supported by the Robert A. Welch Foundation and Texas A&M University. The SQUID magnetometer and EPR spectrometer were acquired with grants from the National Science Foundation (Grant No. CHE-9974899 and Grant No. CHE-1228325, respectively). C.A.M. also thanks the National Science Foundation for IR/D support. The authors are also grateful for the preliminary work by Chun Lin and Shu-Yan Yu.

■ REFERENCES

(1) For example, see: (a) Chisholm, M. H., Ed. *Early Transition Metal Clusters with pi-Donor Ligands*; VCH: New York, 1995. (b) Shriver, D. F., Kaesz, H. D., Adams, R. D., Eds. *The Chemistry of Metal Cluster Complexes*; VCH: New York, 1990. (c) Cotton, F. A.; Wilkinson, G.; Murillo, C. A.; Bochmann, M. *Advanced Inorganic Chemistry*; Wiley: New York, 1999. (d) Vogeley, N. J.; Templeton, J. L. *Polyhedron* **2004**, *23*, 311. (e) D'Souza, F.; Ito, O. *Chem. Commun.* **2009**, 4913. (f) Schneider, H.-J. *Angew. Chem., Int. Ed.* **2009**, *48*, 3924. (g) Vignolle, J.; Cattoen, X.; Bourissou, D. *Chem. Rev.* **2009**, *109*, 3333. (h) Bellachioma, G.; Ciancaleoni, G.; Zuccaccia, C.; Zuccaccia, D.; Macchioni, A. *Coord. Chem. Rev.* **2008**, *252*, 2224. (i) Holland, P. L. *Acc. Chem. Res.* **2008**, *41*, 905. (j) Hay, B. P.; Bryantsev, V. S. *Chem. Commun.* **2008**, 2417. (k) Schottel, B. L.; Chifotides, H. T.; Dunbar, K. R. *Chem. Soc. Rev.* **2008**, *37*, 68. (l) Hembury, G. A.; Borovkov, V. V.; Inoue, Y. *Chem. Soc. Rev.* **2008**, *37*, 1. (m) Petrukhina, M. A. *Coord. Chem. Rev.* **2007**, *251*, 1690. (n) Gamez, P.; Mooibroek, T. J.; Teat, S. J.; Reedijk, J. *Acc. Chem. Res.* **2007**, *40*, 435. (o) Chisholm, M. H. *Proc. Natl. Acad. Sci. U.S.A.* **2007**, *104*, 2563. (p) Conradie, J.; Tangen, E.; Ghosh, A. *J. Inorg. Biochem.* **2006**, *100*, 707. (q) Omary, M. A.; Mohamed, A. A.; Rawashdeh-Omary, M. A.; Fackler, J. P., Jr. *Coord. Chem. Rev.* **2005**, *249*, 1372. (r) Sakaki, S.; Biswas, B.; Musashi, Y.; Sugimoto, M. *J. Organomet. Chem.* **2000**, *611*, 288.

(2) (a) Cotton, F. A.; Murillo, C. A.; Reibenspies, J. H.; Wang, X.; Wilkinson, C. C. *Inorg. Chem.* **2004**, *43*, 8373. (b) Angaridis, P.; Cotton, F. A.; Murillo, C. A.; Villagrán, D.; Wang, X. *J. Am. Chem. Soc.* **2005**, *127*, 5008.

(3) (a) Stephenson, T. A.; Wilkinson, G. *J. Inorg. Nucl. Chem.* **1966**, *28*, 2285. (b) Bennett, M. J.; Caulton, K. G.; Cotton, F. A. *Inorg. Chem.* **1969**, *8*, 1.

(4) Norman, J. G.; Renzoni, G. E.; Case, D. A. *J. Am. Chem. Soc.* **1979**, *101*, 5256.

(5) Angaridis, P. In *Multiple Bonds between Metal Atoms*; Cotton, F. A., Murillo, C. A., Walton, R. A., Eds; Springer Science and Business Media, Inc.: New York, 2005; Ch. 9.

(6) (a) Aquino, M. A. S. *Coord. Chem. Rev.* **2004**, *248*, 1025. (b) Aquino, M. A. S. *Coord. Chem. Rev.* **1998**, *170*, 141. (c) Bear, J. L.; Han, B.; Huang, S.; Kadish, K. M. *Inorg. Chem.* **1996**, *35*, 3012. (d) Chiarella, G. M.; Cotton, F. A.; Murillo, C. A.; Young, M. D.; Zhao, Q. *Inorg. Chem.* **2010**, *49*, 3051. (e) Lee, R.; Yang, Y. Y.; Tan, G. K.; Tan, C.-H.; Wang, K.-W. *Dalton Trans.* **2010**, *39*, 723. (f) Pap, J. S.; Snyder, J. L.; Piccoli, P. M. B.; Berry, J. F. *Inorg. Chem.* **2009**, *48*, 9846. (g) Pap, J. S.; DeBeer George, S.; Berry, J. F. *Angew. Chem., Int. Ed.* **2008**, *47*, 10102. (h) Cummings, S. P.; Savchenko, J.; Fanwick, P. E.; Kharlamova, A.; Ren, T. *Organometallics* **2013**, *32*, 1129. (i) Savchenko, J.; Fanwick, P. E.; Hope, H.; Gao, Y.; Yerneni, C. K.; Ren, T. *Inorg. Chim. Acta* **2013**, *396*, 144. (j) Boudreau, L. J.; Clarke, T. L.; Murray, A. H.; Robertson, K. N.; Cameron, T. S.; Aquino, M. A. S. *Inorg. Chim. Acta* **2013**, *394*, 152.

(7) See for example: (a) Telser, J.; Drago, R. S. *Inorg. Chem.* **1984**, *23*, 3114. (b) Cukiernik, F. D.; Luneau, D.; Marchon, J.-C.; Maldavi, P. *Inorg. Chem.* **1998**, *37*, 3698. (c) Jiménez-Aparicio, R.; Urbanos, F. A.; Arrieta, J. M. *Inorg. Chem.* **2001**, *40*, 613. (d) Handa, M.; Sayama, Y.; Mikuriya, M.; Nukuda, R.; Hiromitsu, I.; Kasuga, K. *Bull. Chem. Soc. Jpn.* **1995**, *68*, 1647. (e) Cheng, W.-Z.; Cotton, F. A.; Dalal, N. S.; Murillo, C. A.; Ramsey, C. M.; Ren, T.; Wang, X. *J. Am. Chem. Soc.* **2005**, *127*, 12691. (f) Liao, Y.; Shum, W. W.; Miller, J. S. *J. Am. Chem. Soc.* **2002**, *124*, 9336. (g) Barral, M. C.; Herrero, S.; Jiménez-Aparicio, R.; Torres, M. R.; Urbanos, F. A. *Angew. Chem., Int. Ed.* **2005**, *44*, 305. (h) Barral, M. C.; Gallo, T.; Herrero, S.; Jiménez-Aparicio, R.; Torres, M. R.; Urbanos, F. A. *Chem.—Eur. J.* **2007**, *13*, 10088. (i) Miyasaka, H.; Motokawa, N.; Matsunaga, S.; Yamashita, M.; Sugimoto, K.; Mori, T.; Toyota, N.; Dunbar, K. *J. Am. Chem. Soc.* **2010**, *132*, 1532. (j) Barral, M. C.; González-Prieto, R.; Herrero, S.; Jiménez-Aparicio, R.; Priego, J. L.; Royer, E. C.; Torres, M. R.; Urbanos, F. A. *Polyhedron* **2004**, *23*, 2637. (k) Delgado, P.; Gonzalez-Prieto, R.; Jiménez-Aparicio, R.; Perles, J.; Priego, J.; Torress, R. M. *Dalton Trans.* **2012**, *41*, 11866. (l) Delgado-Martínez, P.; González-Prieto, R.; Gómez-García, C. J.; Jiménez-Aparicio, R.; Priego, J. L.; Torres, M. R. *Dalton Trans.* **2014**, *43*, 3227. (m) Haque, F.; del Barco, E.; Fishman, R. S.; Miller, J. S. *Polyhedron* **2013**, *64*, 73. (n) Da Silva, J. G.; Miller, J. S. *Inorg. Chem.* **2013**, *52*, 1418. (o) Her, J.-H.; Stephens, P. W.; Kennon, B. S.; Liu, C.; Miller, J. S. *Inorg. Chim. Acta* **2010**, *364*, 172. (p) Ikeue, T.; Kimura, Y.; Karino, K.; Iida, M.; Yamahi, T.; Hiromitsu, I.; Sugimori, T.; Yoshioka, D.; Mikuriya, M.; Handa, M. *Inorg. Chem. Commun.* **2013**, *33*, 133.

(8) For an account of electronic configurations in paddlewheel compounds, see: Falvello, L. R.; Foxman, B. M.; Murillo, C. A. *Inorg. Chem.* **2014**, *53*, in press. dx.doi.org/10.1021/ic500119h.

(9) The chemical composition of this system is $[Ru_2(OAc)(DPhF)_3(H_2O)](SO_3CF_3)\cdot THF$. In both paddlewheel molecules there is an axial water molecule that is hydrogen-bonded to a triflate anion, but in only one of the Ru_2^{5+} species there is a hydrogen-bonded interaction between water and the THF molecule. For the latter, the Ru−Ru distances are 2.3637(6) Å at 30 K and 2.3255(5) Å at 298 K, and for the molecule that is devoid of hydrogen bonded interactions to the THF molecule these distances are 2.2950(6) Å and 2.3064(5) Å, respectively. See: Cotton, F. A.; Herrero, S.; Jiménez-Aparicio, R.; Murillo, C. A.; Urbanos, F. A.; Villagrán, D.; Wang, X. *J. Am. Chem. Soc.* **2007**, *129*, 12666.

(10) For references on noncoordinating anions, see, for example: (a) Krossing, I.; Raabe, I. *Angew. Chem., Int. Ed.* **2004**, *43*, 2066 and the references therein. (b) Rach, S. F.; Kühn, F. E. *Chem. Rev.* **2009**, *109*, 2061. (c) Adams, H.; Fenton, D. E.; McHugh, P. E.; Potter, T. *Inorg. Chim. Acta* **2002**, *331*, 117. (d) Sharma, R. P.; Singh, A.; Venugopalan, P.; Harrison, W. T. A. *J. Mol. Struct.* **2011**, *994*, 6. (e) Reisinger, A.; Trapp, N.; Knapp, C.; Himmel, D.; Breher, F.; Ruegger, H.; Krossing, I. *Chem.—Eur. J.* **2009**, *15*, 9505. (f) Barriere, F.; Geiger, W. E. *J. Am. Chem. Soc.* **2006**, *128*, 3980.

(11) The use of a noncoordinating solvent is essential. Many compounds having Ru_2^{5+} cores with BF_4 or other noncoordinating counterions are known, but without exception they contain axial ligands such as H_2O, acetonitrile, and other coordinating neutral species. For examples, see: (a) Bino, A.; Cotton, F. A.; Felthouse, T. R. *Inorg. Chem.* **1979**, *18*, 2599. (b) Cotton, F. A.; Lu, J.; Yokochi, A. *Inorg. Chim. Acta* **1998**, *275*−*276*, 447. (c) Anez, E.; Herrero, S.; Jiménez-Aparicio, R.; Priego, J. L.; Torres, M. R.; Urbanos, F. A. *Polyhedron* **2010**, *29*, 232. (d) Barral, M. C.; Herrero, S.; Jiménez-Aparicio, R.; Priego, J. L.; Torres, M. R.; Urbanos, F. A. *J. Mol. Struct.* **2008**, *890*, 221. (e) Barral, M. C.; Gallo, T.; Herrero, S.; Jiménez-Aparicio, R.; Torres, M. R.; Urbanos, F. A. *Chem.—Eur. J.* **2007**, *13*, 10088. (f) Chisholm, M. H.; Christou, G.; Folting, K.; Huffman, J. C.; James, C. A.; Samuels, J. A.; Wesemann, J. L.; Wooddruff, W. H. *Inorg. Chem.* **1996**, *35*, 3643. (g) Furakawa, S.; Kitagawa, S. *Inorg. Chem.* **2004**, *43*, 6464.

(12) For additional information on substituents effects on dinuclear paddlewheel compounds and Hammett σ constants for DAniF species, see: Ren, T. *Coord. Chem. Rev.* **1998**, *175*, 43.

(13) For reference, the closest approach of a fluorine atom to a ruthenium atom is over 4.7 Å. The Ru(1)···F(3A) separation is 4.74(1), 4.75(1), and 5.04(2) Å at 200, 298, and 27 K, respectively.

(14) To our knowledge there is only one structure of a compound with an Ru_2^{5+} core that is devoid of an axial ligand ($Ru_2(DPhF)_3Br_2$), but this is not a paddlewheel species. This compound has a dimetal core spanned by the bridging formamidinate bridges. The remaining equatorial positions are occupied by the two halide species. The Ru−Ru distance is 2.4011(4) Å and its magnetism is intermediate between that that is expected from either species with three or one unpaired electron. See: Barral, M. C.; Gallo, T.; Herrero, S.; Jiménez-Aparicio, R.; Torres, M. R.; Urbanos, F. A. *Chem.—Eur. J.* **2007**, *13*, 10088.

(15) Barral, M. C.; González-Prieto, R.; Jiménez-Aparicio, R.; Priego, J. L.; Torres, M. R.; Urbanos, F. A. *Eur. J. Inorg. Chem.* **2003**, 2339 and the references therein.

(16) The magnetic data for **2**, which is similar to that of diruthenium tetracarboxylates, show a highly anisotropic behavior with a strong ZFS, which can be modeled using the following set of equations:

$$\chi_{\parallel} = \frac{N g_{\parallel}^{\,2} \beta^2}{kT} \frac{1 + 9\exp\left(-\frac{2D}{kT}\right)}{4\left[1 + \exp\left(-\frac{2D}{kT}\right)\right]}$$

$$\chi_{\perp} = \frac{N g_{\perp}^{\,2} \beta^2}{kT} \frac{4 + \left(\frac{3kT}{D}\right)\left[1 - \exp\left(-\frac{2D}{kT}\right)\right]}{4\left[1 + \exp\left(-\frac{2D}{kT}\right)\right]}$$

where $\chi = (\chi_{\parallel} + 2\chi_{\perp})/3$, N is Avogadro's number, D is the ZFS parameter in cm^{-1}, β is the Bohr magneton, k is the Boltzmann constant, and T is the temperature in Kelvin. The modeling of the data of **2** with these equations yields anisotropic values of $g_{\parallel}$ and $g_{\perp}$ of 1.72(4) and 2.02(1), respectively, which are consistent with the EPR data (vide supra), and the value of D of 75(3) is consistent to that of similar diruthenium complexes.

(17) The crystal structure of **1** has interstitial CH_2Cl_2 with an occupancy of 0.5, which plays no role in its structure since it resides in a noncoordinating position away from the axial location.

(18) Kondo, M.; Hamatami, M.; Kitagawa, S. *J. Am. Chem. Soc.* **1998**, *120*, 455.

(19) For large values of D and $S = {}^3/_2$, the effective (g^e) and actual g-values are related by $g_{\perp} = g_{\perp}^e/2$ and $g_{\parallel} = g_{\parallel}^e$. See ref 7e or Pilbrow, J. R. *J. Mag. Res.* **1978**, *31*, 479. In addition, $g_{iso} = (2g_{\perp} + g_{\parallel})/3$.

(20) *Multiple Bonds between Metal Atoms*; Cotton, F. A., Murillo, C. A., Walton, R. A., Eds.; Springer Science and Business Media, Inc.: New York, 2005.

(21) Cotton, F. A.; Hillard, E. A.; Murillo, C. A.; Zhou, H.-C. *J. Am. Chem. Soc.* **2000**, *122*, 416.

(22) Cotton, F. A.; Hillard, E. A.; Liu, C. Y.; Murillo, C. A.; Wang, W.; Wang, X. *Inorg. Chim. Acta* **2002**, *337*, 233.

(23) Cotton, F. A.; Hillard, E. A.; Murillo, C. A. *J. Am. Chem. Soc.* **2002**, *124*, 5658.

(24) Cotton, F. A.; Daniels, L. M.; Murillo, C. A.; Pascal, I.; Zhou, H.-C. *J. Am. Chem. Soc.* **1999**, *121*, 6856.

(25) Cotton, F. A.; Donahue, J. P.; Lichtenberger, D. L.; Murillo, C. A.; Villagrán, D. *J. Am. Chem. Soc.* **2005**, *127*, 10808.

(26) Cotton, F. A.; Donahue, J. P.; Gruhn, N. E.; Lichtenberger, D. L.; Murillo, C. A.; Timmons, D. J.; Van Dorn, L. O.; Villagrán, D.; Wang, X. *Inorg. Chem.* **2006**, *45*, 201.

(27) Chiarella, G. M.; Cotton, F. A.; Murillo, C. A.; Young, M. D. *Inorg. Chem.* **2011**, *50*, 1258.

(28) Barral, M. C.; Herrero, S.; Jiménez-Aparicio, R.; Torres, M. R.; Urbanos, F. A. *Inorg. Chem. Commun.* **2004**, *7*, 42.

(29) Angaridis, P.; Cotton, F. A.; Murillo, C. A.; Wang, X. *Acta Crystallogr.* **2005**, *C61*, m71.

(30) Barral, M. C.; Casanova, D.; Herrero, S.; Jiménez-Aparicio, R.; Torres, M. R.; Urbanos, F. A. *Chem.—Eur. J.* **2010**, *16*, 6203.

(31) See, for example: Liu, I. P.-C.; Ren, T. *Inorg. Chem.* **2009**, *48*, 5608.

(32) Even though the calculated absolute value may not fully agree, the trend (see text) is relevant.
(33) Note that the σ and σ^* orbitals also drop in energy because of the symmetry-allowed σ–L interaction, but this drop in energy does not affect the overall multiplicity of the systems as the π interaction does.
(34) The calculated Ru–Ru distances according to the DFT optimized models closely resemble the experimentally observed bond distances. The calculated Ru–Ru bond distance for the doublet model without an axial ligand is 2.4138 Å, which is in close agreement with the Ru–Ru distance of **3**, 2.4000(5) Å and of **4**, 2.3859(4) Å. In contrast, the calculated quartet Ru_2-Cl model has a Ru–Ru bond distance of 2.36165 Å, which is similar than those of **1**, 2.3968(5) and **2**, 2.3398 (4) Å.
(35) (a) Cotton, F. A.; Daniels, L. M.; Murillo, C. A.; Schooler, P. *Dalton Trans.* **2000**, 2007. (b) Mohamed, A. A.; Abdou, H. E.; Irwin, M. D.; López-de-Luzuriaga, J. M.; Fackler, J. P., Jr. *J. Cluster Sci.* **2003**, *14*, 253.
(36) Mitchell, R. W.; Spencer, A.; Wilkinson, G. *J. Chem. Soc., Dalton Trans.* **1973**, 846.
(37) Angaridis, P.; Cotton, F. A.; Murillo, C. A.; Villagrán, D.; Wang, X. *Inorg. Chem.* **2004**, *43*, 8290–8300.
(38) *Theory and Applications of Molecular Paramagnetism*; Boudreaux, E. A., Mulay, L. N., Eds.; John Wiley and Sons: New York, 1976.
(39) (a) Hohenberg, P.; Kohn, W. *Phys. Rev.* **1964**, *136*, B864. (b) *Density-Functional Theory of Atoms and Molecules*; Parr, R. G., Yang, W., Eds.; Oxford University Press: Oxford, UK, 1989.
(40) (a) Becke, A. D. *Phys. Rev. A* **1988**, *38*, 3098. (b) Becke, A. D. *J. Chem. Phys.* **1993**, *98*, 1372. (c) Becke, A. D. *J. Chem. Phys.* **1993**, *98*, 5648.
(41) Lee, C. T.; Yang, W. T.; Parr, R. G. *Phys. Rev. B* **1998**, *37*, 785.
(42) Frisch, M. J.; Trucks, G. W.; Schlegel, H. B.; Scuseria, G. E.; Robb, M. A.; Cheeseman, J. R.; Montgomery, J. A., Jr.; Vreven, T.; Kudin, K. N.; Burant, J. C.; Millam, J. M.; Iyengar, S. S.; Tomasi, J.; Barone, V.; Mennucci, B.; Cossi, M.; Scalmani, G.; Rega, N.; Petersson, G. A.; Nakatsuji, H.; Hada, M.; Ehara, M.; Toyota, K.; Fukuda, R.; Hasegawa, J.; Ishida, M.; Nakajima, T.; Honda, Y.; Kitao, O.; Nakai, H.; Klene, M.; Li, X.; Knox, J. E.; Hratchian, H. P.; Cross, J. B.; Bakken, V.; Adamo, C.; Jaramillo, J.; Gomperts, R.; Stratmann, R. E.; Yazyev, O.; Austin, A. J.; Cammi, R.; Pomelli, C.; Ochterski, J. W.; Ayala, P. Y.; Morokuma, K.; Voth, G. A.; Salvador, P.; Dannenberg, J. J.; Zakrzewski, V. G.; Dapprich, S.; Daniels, A. D.; Strain, M. C.; Farkas, O.; Malick, D. K.; Rabuck, A. D.; Raghavachari, K.; Foresman, J. B.; Ortiz, J. V.; Cui, Q.; Baboul, A. G.; Clifford, S.; Cioslowski, J.; Stefanov, B. B.; Liu, G.; Liashenko, A.; Piskorz, P.; Komaromi, I.; Martin, R. L.; Fox, D. J.; Keith, T.; Al-Laham, M. A.; Peng, C. Y.; Nanayakkara, A.; Challacombe, M.; Gill, P. M. W.; Johnson, B.; Chen, W.; Wong, M. W.; Gonzalez, C.; Pople, J. A. *Gaussian 03*, revision B.05; Gaussian, Inc.: Wallingford, CT, 2003.
(43) Dunning, T. H.; Hay, P. J. In *Modern Theoretical Chemistry. 3. Methods of Electronic Structure Theory*; Schaefer, H. F., III, Ed.; Plenum Press: New York, 1977; pp 1–28.
(44) (a) Wadt, W. R.; Hay, P. J. *J. Chem. Phys.* **1985**, *82*, 284. (b) Wadt, W. R.; Hay, P. J. *J. Chem. Phys.* **1985**, *82*, 299.
(45) Couty, M.; Hall, M. B. *J. Comput. Chem.* **1996**, *17*, 1359.
(46) *SMART for Windows NT*, version 5.618; Bruker Advanced X-ray Solutions, Inc.: Madison, WI, 2001.
(47) *SAINT. Data Reduction Software*, version 6.36A; Bruker Advanced X-ray Solutions, Inc.: Madison, WI, 2001.
(48) *SADABS. Area Detector Absorption and other Corrections Software*, version 2.05; Bruker Advanced X-ray Solutions, Inc.: Madison, WI, 2001.
(49) Sheldrick, G. M. *SHELXTL*, version 6.12; Bruker Advanced X-ray Solutions, Inc.: Madison, WI, 2002.
(50) Marsh, R. E. *Acta Crystallogr.* **2009**, *B65*, 782.